Acta Pharmacologica Sinica

www.nature.com/aps

ARTICLE

Uncarboxylated osteocalcin ameliorates hepatic glucose and lipid metabolism in KKAy mice via activating insulin signaling pathway

Xiao-lin Zhang[1,2], Ya-nan Wang[2], Lu-yao Ma[1], Zhong-sheng Liu[1], Fei Ye[2] and Jian-hong Yang[1]

Osteocalcin, expressed in osteoblasts of the bone marrow, undergoes post-translational carboxylation and deposits in mineralized bone matrix. A portion of osteocalcin remains uncarboxylated (uncarboxylated osteocalcin, GluOC) that is released into blood where it functions as a hormone to regulate insulin secretion and insulin sensitivity. As insulin resistance is closely associated with metabolic syndrome, this study is aimed to elucidate how GluOC regulates glucose and lipid metabolism in KKAy mice, an animal model displaying obese, hyperglycemia, hyperinsulinemia, insulin resistance, and hepatic steatosis. GluOC (3, 30 ng/g per day, ig) was orally administered to female KKAy mice for 4 weeks. Whole-body insulin sensitivity, glucose metabolism, hepatic steatosis, dyslipidemia were examined using routine laboratory assays. We found that GluOC administration significantly enhanced insulin sensitivity in KKAy mice by activating hepatic IRβ/PI3K/Akt pathway and elevated the whole-body insulin sensitivity with decreased FPI and HOMA-IR index. Furthermore, GluOC administration alleviated hyperglycemia through suppressing gluconeogenesis and promoting glycogen synthesis in KKAy mice and in cultured hepatocytes in vitro. Moreover, GluOC administration dose-dependently ameliorated dyslipidemia and attenuated hepatic steatosis in KKAy mice by inhibiting hepatic de novo lipogenesis and promoting fatty-acid β-oxidation. These results demonstrate that GluOC effectively enhances hepatic insulin sensitivity, improves hyperglycemia and ameliorates hepatic steatosis in KKAy mice, suggesting that GluOC could be a promising drug candidate for treating metabolic syndrome.

Keywords: metabolic syndrome; uncarboxylated osteocalcin (GluOC); insulin resistance; hyperglycemia; dyslipidemia; non-alcoholic fatty-liver disease (NAFLD); obese; KKAy mouse

Acta Pharmacologica Sinica (2020) 41:383–393; https://doi.org/10.1038/s41401-019-0311-z

INTRODUCTION

Metabolic syndrome (MetS) is a cluster of metabolic abnormalities, including obesity, type 2 diabetic mellitus (T2DM), and dyslipidemia. The prevalence of both obesity and MetS continues to rise worldwide. Non-alcoholic fatty-liver disease (NAFLD) consists of a spectrum of chronic liver disorders from simple hepatic steatosis, steatohepatitis, and fibrosis to cirrhosis, and even carcinoma. NAFLD is expected to become the most common cause of chronic liver diseases, may be affecting >30% of the general population [1]. NAFLD may be viewed as a hepatic form of MetS [2–5]. Glucose and triglycerides (TG) represent two key Mets components, and a fatty liver may secrete more glucose and TG in addition to hepatic accumulation. The liver is therefore a key participant in metabolic abnormalities [6]. Insulin resistance is progressively recognized as a link between MetS and NAFLD [3, 7, 8] and is associated with excessive lipid accumulation in the liver (steatosis), which may further augment insulin resistance. This favors the use of insulin sensitizers for treating both MetS and NAFLD.

The drug targets for insulin sensitizers include PPARγ [9] and PTP1B [10]. PPARγ agonists are not on the recommendation list, while PTP1B inhibitors need regulatory approval for clinical applications. Accumulated evidence over the last decade suggests that bone also functions as an endocrine organ regulating whole-body glucose and energy metabolism. Osteoblasts in the bone marrow express osteocalcin, which undergoes post-translational carboxylation and deposits in mineralized bone matrix. A portion of osteocalcin remains uncarboxylated (uncarboxylated osteocalcin, GluOC) and can be released into blood, where it functions as a hormone to regulate insulin secretion and insulin sensitivity [11–13]. For instance, elevated blood glucose, impaired glucose tolerance, insulin resistance, lower energy expenditure, and impaired β-cell function were observed in osteocalcin knockout mice ($Ocn^{-/-}$) [12]. Osteocalcin exerts its biological function by binding to G protein-coupled receptor family C member A (GPRC6A) in target organs. GPRC6A involvement was demonstrated by $GPRC6A^{-/-}$ mice, which displayed the phenotype of hepatic steatosis, hyperglycemia, glucose intolerance, and insulin resistance [14]. An increase in the serum osteocalcin level through administration of exogenous osteocalcin mitigated obesity and glucose intolerance in chow- or high-fat diet (HFD)-fed mice [15–17]. It has been accepted that the insulin sensitivity in adipose tissue and muscle could be increased by osteocalcin, but its insulin-sensitizing function in the liver remains to be established [11, 18]. Osteocalcin reduced hepatic steatosis in high-fat diet-fed wild-type mice or high-fat and high-cholesterol diet

[1]Medical School, University of Chinese Academy of Sciences, Beijing 101400, China and [2]Beijing Key Laboratory of New Drug Mechanisms and Pharmacological Evaluation Study, Institute of Materia Medica, Chinese Academy of Medical Sciences & Peking Union Medical College, Beijing 100050, China
Correspondence: Fei Ye (yefei@imm.ac.cn) or Jian-hong Yang (yangjh@ucas.edu.cn)

Received: 8 March 2019 Accepted: 19 September 2019
Published online: 28 October 2019

(WHFD)-fed *Ldlr*$^{-/-}$ male mice [16, 19]. However, these studies did not characterize the mechanisms by which osteocalcin regulated glucose and lipid metabolism in the liver.

In this study, we tested the impact of GluOC on glucose and lipid metabolism in KKAy mice, a T2DM animal model of MetS that displays obesity, hyperglycemia, hyperinsulinemia, insulin resistance, and hepatic steatosis [20]. Fascinatingly, KKAy mice had significantly lower serum GluOC than C57BL/6 mice, as demonstrated by our earlier study [21], suggesting a GluOC deficiency that may underlie the abnormal phenotype. Our results confirmed that GluOC treatment made hepatocytes more responsive to insulin and improved glucose and lipid metabolism in KKAy mice.

MATERIALS AND METHODS

Chemicals and reagents

Recombinant mouse GST-osteocalcin fusion protein was expressed in BL21 (DE3) (TransGen Biotech, Beijing, China) with the expression plasmid pGEX-6p-1, which encodes human BGLAP2. GST-osteocalcin fusion protein in the bacterial extract was purified using Glutathione Sepharose 4B (GE Healthcare Life Sciences, Piscataway Township, NJ, USA) and cleaved from the GST moiety using PreScission Protease. Then the digested sample was loaded onto Glutathione Sepharose 4B again to remove GST and GST-osteocalcin fusion protein. The GE AKTA Purifier Purification system was used for purification procedures. The relative purity of the osteocalcin was assessed by sodium dodecyl sulfate-polyacrylamide gel electrophoresis (SDS-PAGE) and Coomassie blue staining. The specificity of the recombinant osteocalcin was probed by osteocalcin antibody (Abcam, Cambridge, MA, USA) after SDS-PAGE separation. For blood uncarboxylated OC level determination, the serum was collected 24 h after the last oral dose of 14-day OC administration, and a Mouse Glu-Osteocalcin High Sensitive EIA Kit (Takara, Tokyo, Japan) was used.

General reagents were purchased from Sigma-Aldrich (St. Louis., MO, USA). Water was obtained using a PALL Cascada™ Lab Water Purification System (Pall Corporation, New York, USA). A mouse insulin ultrasensitive ELISA kit was purchased from ALPCO (Salem, NH, USA). The ECL reaction kit was obtained from Tanon Science & Technology (Shanghai, China). Cell culture media were supplied by GIBCO (Grand Island, NY, USA). The following antibodies were used to determine the activity of the insulin signaling pathway and hepatic lipid metabolism pathway: β-actin, GAPDH, fatty acid synthase (FAS), acetyl-CoA carboxylase (ACC), insulin receptor β (IRβ), protein kinase B (PKB/Akt), Akt (pS473), forkhead box O1 (Foxo1), Foxo1 (pS256), glycogen synthase kinase 3 beta (GSK3β), and GSK3β (pS9) from Cell Signaling Technology (Danvers, MA, USA); cluster of differentiation 36 (CD36), carnitine palmitoyltransferase I (CPT1), and medium-chain acyl-CoA dehydrogenase (MCAD) from Abcam; and SREBP1c and IRβ (pY1162/1163) from Santa Cruz Biotechnology (Santa Cruz, CA, USA).

Animals and OC treatment

The Animal Center of the Institute of Laboratory Animal Sciences, Chinese Academy of Medical Sciences (CAMS), and Peking Union Medical College (PUMC) [license number: SCXK (Jing) 2014-0004] supplied all experimental animals for this study. Mice were housed in grommet cages (five mice per cage) under the conditions of temperature 21–23 °C, humidity 40%–60%, 12 h light/dark cycle, and ad libitum access to water and chow diet. Standard protocols were followed to minimize animal discomfort throughout experiments. All animal procedures followed the Revised International Guiding Principles for Biomedical Research Involving Animals and Animal Welfare Assurances for Foreign Institutions established by the National Institutes of Health (NIH, USA). Animal protocols were approved by the Institutional Animal Care and Use Committee of CAMS & PUMC.

The 18-week-old female KKAy mice with an average weight of 50 g were fed a chow diet (1K65, Beijing HFK Bioscience Co. Ltd., China) and randomly divided into three groups ($n = 10$): phosphate buffered saline (PBS) control, OC-L (3 ng/g body weight/day) and OC-H (30 ng/g body weight/day). Nonfasting glucose, fasting glucose, and body weight were measured before treatment. As shown in Table 1, there were no significant differences in the three markers among the three groups. PBS and GluOC were orally administered daily for 4 weeks. Aged-matched female C57BL/6 mice fed a standard chow diet (1022, Beijing HFK Bioscience Co. Ltd., China) were orally administered PBS (0.1 mL/10 g body weight) as a normal control (C57).

Table 1. Body weight and blood glucose before GluOC treatment ($n = 10$)

	KKAy	OC-L	OC-H
Nonfasting glucose (mg/dL)	432.1 ± 52.7	429.6 ± 37.1	429.6 ± 47.2
Fasting glucose (mg/dL)	256.6 ± 76.4	257.1 ± 74.0	256.6 ± 79.9
Body weight (g)	50.3 ± 2.7	50.5 ± 2.0	49.6 ± 2.0

Glucose metabolism evaluation in mice

During administration, nonfasting blood glucose and fasting blood glucose (FBG) were kinetically monitored at days 0, 7, 14, and 24 of GluOC administration. An oral glucose tolerance test (OGTT) was performed on day 28. Blood samples were collected from tails for determination of baseline values of blood glucose (0 min) after 4-h fasting. The mice were then orally administered glucose (2 g/kg body weight), and blood samples were collected at 15, 60, and 120 min. A glucose oxidase (GOD) assay was used for blood glucose level measurement. The values of the area under the glucose-time curve (AUC) were calculated.

Insulin sensitivity estimation in mice

After GluOC administration for 14 days, the fasting plasma insulin (FPI) was determined. The Homeostatic Model Assessment of Insulin Resistance (HOMA-IR) index was calculated with the following formula: HOMA-IR index = (FPI × FPG)/22.5, where FPI is fasting plasma insulin concentration (mU/L) and FPG is fasting plasma glucose (mM) [22]. Animals were fasted for 4 h before FPI/FPG determination.

Evaluation of hepatic lipid accumulation

After 4 weeks of GluOC treatment, hepatic histology and TG content were evaluated in KKAy mice. Hematoxylin and eosin-stained liver sections were used for histology evaluation. The scope of steatosis was scored as 0 (no steatosis), 1 (< 25% of hepatocytes), 2 (26%–50%), 3 (51%–75%), and 4 (> 75%) [23]. Hepatic TG was extracted from the left lateral lobe of the liver per the published method [24] and determined with commercial biochemical kits (Biosino Biotechnology Co., Ltd., Beijing, China).

Evaluation of blood lipid panel

Blood samples were collected from the tails after 4 h of fasting. Serum levels of TG, total cholesterol (TC), high-density lipoprotein cholesterol (HDL-C), and low-density lipoprotein cholesterol (LDL-C) were quantitatively detected with commercial kits (Biosino Biotechnology Co., Ltd., Beijing, China).

Analysis of hepatic insulin and glucose metabolism pathways

After 4 weeks of GluOC treatment, mice were first fasted overnight and then anesthetized by intraperitoneal injection of 1% sodium pentobarbital (0.1 mL/10 g). Five animals in each group were randomly selected and injected with quick-acting insulin (Lispro, Eli Lilly and Co., Indianapolis, Indiana, USA) 1 U/kg into the inferior vena cava, and the liver was separated 3 min after insulin injection and immediately frozen in liquid nitrogen. The other five mice

underwent the same sham operation without insulin injection. Livers were homogenized in ice-cold RIPA lysis buffer [50 mM Tris-HCl, 150 mM NaCl, 1% NP-40, 0.1% SDS, protease inhibitor cocktail, and PhosSTOP at pH 7.4 (Roche, Basel, Switzerland)]. Western blot was conducted to detect the expression of proteins related to hepatic insulin and glucose metabolism pathways as previously described [25]. The images were acquired on a Tanon-5200 Chemiluminescent Imaging System (Tanon Science & Technology, Shanghai, China).

Analysis of hepatic lipid metabolism pathways

After 4 weeks of GluOC treatment, liver tissues were removed under anesthetization conditions from mice after overnight fasting for protein analysis. Total proteins from liver lysates were separated by SDS-PAGE, transferred to polyvinylidene difluoride membranes (Merck Millipore, Billerica, Massachusetts, USA), and then probed with anti-SREBP1c, FAS, ACC, CPT1, MCAD, and CD36 antibodies.

Evaluation of glucose metabolism in primary cultured hepatocytes

Mouse primary hepatocytes were prepared using the established procedure [26]. Briefly, the livers from male C57BL/6 mice were retrograde-perfused using collagenase I (Sigma-Aldrich, St. Louis., MO, USA) through the inferior vena cava under anesthesia to isolate primary hepatocytes. Trypan blue staining was used to estimate cell viability. The isolated cells with viability > 95% were eligible for plating.

For the glucose output assay, hepatocytes were seeded in six-well plates and incubated for 24 h in Williams' medium E supplemented with 100 μg/mL penicillin and 100 U/mL streptomycin, 1% (*v*/*v*) 200 mM *L*-glutamine (Sigma), and 10% (*v*/*v*) fetal bovine serum. Then cells were treated with GluOC (0, 3, 30 ng/mL) for 24 h, washed with PBS and incubated in glucose production medium (glucose- and phenol red-free Dulbecco's Modified Eagle's Medium, containing 2 mM sodium pyruvate and 20 mM sodium lactate) for 4 h. The medium was harvested to measure the glucose concentration.

To evaluate the impact of GluOC on glycogen synthesis, cells were serum-starved for 6 h and then treated with GluOC (0, 3, 30 ng/mL) for 24 h followed by 10 nM insulin treatment for 5 min. The phosphorylation of GSK3β was determined by immunoblotting.

Liquid chromatography-tandem mass spectrometry (LC-MS/MS) analysis of mouse liver samples

Total liver proteins were isolated from individual mouse livers ($n = 3$ for the KKAy and OC-L groups) using the SDT buffer (4% SDS, 100 mM DTT, 150 mM Tris-HCl pH 7.6). Each protein sample was subjected to the filter-aided sample preparation (FASP) described by Wisniewski [27] and digestion. The peptide mixture was transferred to a reverse-phase trap column (Thermo Scientific Acclaim PepMap100, 100 μm × 2 cm, nanoViper C18) that was coupled with a C18 reversed-phase analytical column (Thermo Scientific Easy Column, 10 cm long, 75-μm inner diameter, 3-μm resin) in buffer A (0.1% formic acid). The mix was separated with buffer B (84% acetonitrile and 0.1% formic acid) at a flow rate of 300 nL/min for 2 h. The label-free quantification was carried out using MaxQuant as previously described [28], and the MS raw data were matched to the UniProt *Mus musculus* database on 4/20/2018. To determine the ontology and biological properties of the identified proteins, the protein sequences were mapped to GO parameters in BLAS-T2GO (Version 3.3.5, BioBam, Valencia, Spain). Proteins that were identified in functional categories and pathways with *P*-values < 0.05 were considered significantly enriched.

Statistical analysis

The data were analyzed by one-way ANOVA. All values are presented as means ± SD or SEM, and statistical significance was considered when $P < 0.05$.

RESULTS

GluOC treatment improves hyperglycemia, glucose intolerance, and whole-body insulin resistance in KKAy mice

The blood uncarboxylated OC levels were ~1.3- and ~1.6-fold higher in the OC-L and OC-H groups compared with the PBS group, respectively (Fig. 1a). Nonfasting and fasting blood glucose (FBG) levels were significantly higher in the PBS-treated KKAy mice compared with C57 mice, and both were significantly lower in the GluOC-treated groups, especially FBG (Fig. 1b, c). A 14-day treatment led FBG to be 20.2% and 21.9% lower in the OC-L and OC-H groups, respectively, compared to the PBS-treated KKAy mice; 27.3% and 26.5% lower FBG was observed after 24-day treatment. In OGTT, the blood glucose levels after glucose loading in the PBS-treated KKAy mice were significantly higher than those in C57 mice (Fig. 1d), which indicated impaired glucose tolerance (IGT). GluOC treatment improved glucose intolerance in the OC-H group, as seen by an ~11% decrease in AUC_{ogtt} (Fig. 1e).

KKAy mice displayed severe insulin resistance, showing significantly higher FPI and HOMA-IR compared with C57 mice. The high FPI and HOMA-IR were both reduced by GluOC treatment (Fig. 1f, g). These findings suggest that treatment with both GluOC doses (3 and 30 ng/g BW) delivered hypoglycemic and insulin-sensitizing effects in KKAy mice.

GluOC treatment prevents hepatic steatosis in KKAy mice

KKAy mice developed prominent hepatocyte lipidosis and hepatic steatosis throughout the entire lobule, and the hepatic cord structure was not distorted. After 4 weeks of GluOC treatment, hepatocyte lipidosis was significantly ameliorated, especially in the OC-H group (Fig. 2a, b). The hepatic TG content in KKAy mice was 10.8-fold higher than in C57 mice. The GluOC treatment significantly lowered the high TG content by as much as 58.3% in the OC-H group (Fig. 2c).

GluOC treatment ameliorates dyslipidemia in KKAy mice by decreasing blood TG and TC levels

KKAy mice developed prominent dyslipidemia, showing higher serum TC, TG, HDL-C, and LDL-C compared with C57 mice. As shown in Fig. 3, the serum TC and TG levels became lower in response to GluOC treatment without altering food intake or body weight in KKAy mice.

GluOC treatment enhances insulin sensitivity by activating the hepatic IRβ/PI3K/Akt pathway in KKAy mice

Insulin function is mediated by activating the insulin receptor and downstream signaling molecules. To understand the underlying mechanisms responsible for the improved insulin sensitivity in GluOC-treated mice, insulin signaling molecules in liver tissues were investigated. As shown in Fig. 4, the insulin signaling pathway was suppressed in KKAy mice, showing a downregulated phosphorylation of IRβ, PI3K, and Akt after insulin administration in C57 mice. After 4 weeks of treatment, the insulin-induced phosphorylation of IRβ and Akt was upregulated in OC-L- and OC-H-treated mice compared with KKAy mice, suggesting that GluOC treatment enhanced the hepatic insulin signaling pathway in KKAy mice.

GluOC treatment ameliorates hyperglycemia by suppressing gluconeogenesis and promoting glycogen synthesis in KKAy mice

The activation of the IRβ/PI3K/Akt pathway was accompanied by upregulated insulin-stimulated phosphorylation of Foxo1 (Ser253) and GSK3β (Ser9), which are involved in glucose metabolism downstream (Fig. 5a–d). Foxo1 is the key transcription factor in gluconeogenesis, and GSK3β is involved in glycogen synthesis. Remarkably, the total Foxo1 expression was significantly higher in KKAy mice but was significantly lower in GluOC-treated mice compared to C57 mice (Fig. 5b). These results suggested that GluOC

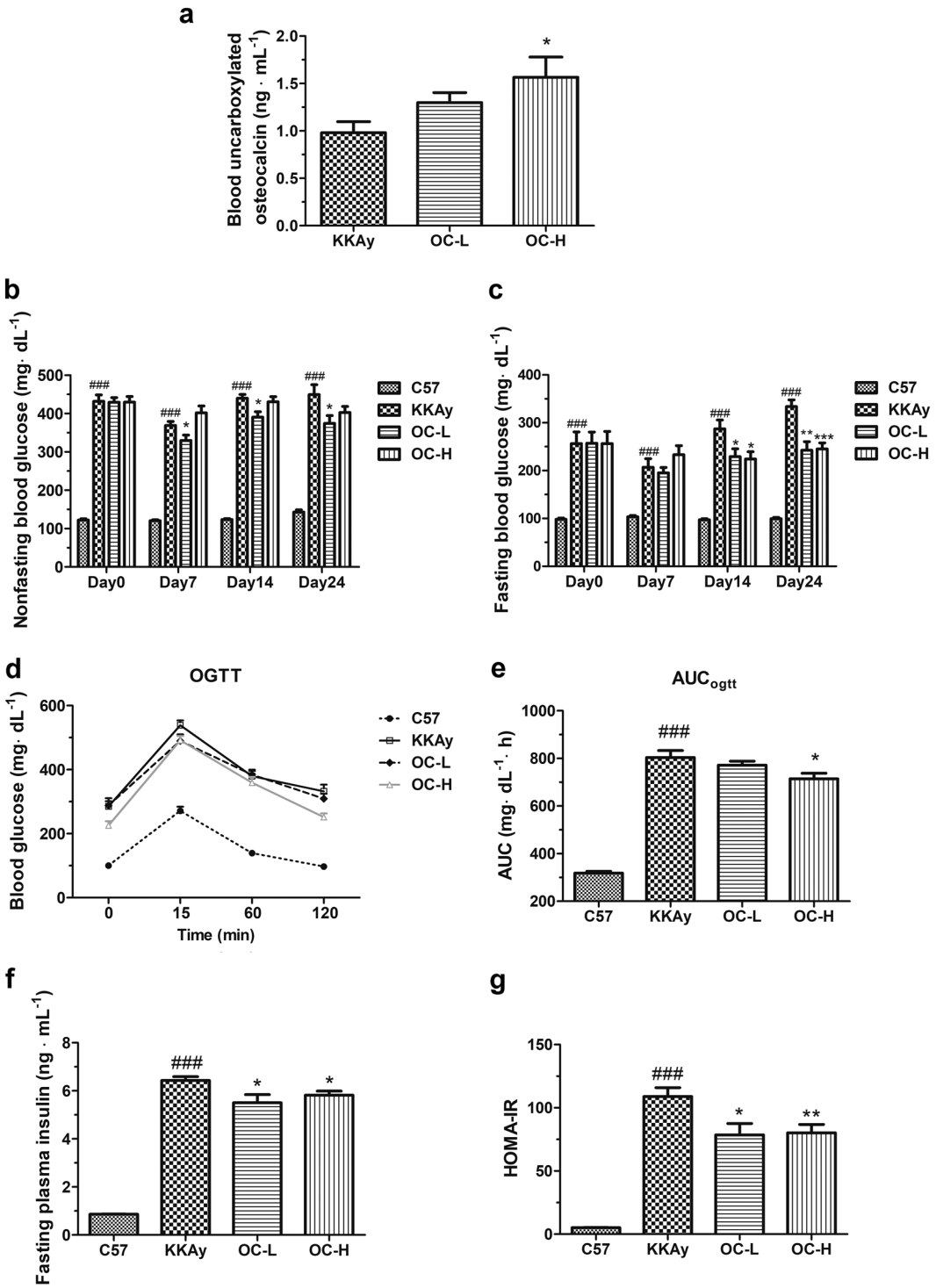

Fig. 1 GluOC treatment improves hyperglycemia, glucose intolerance, and whole-body insulin resistance in KKAy mice. Animals were treated with GluOC (3 or 30 ng/g BW) for 28 days. **a** Blood uncarboxylated osteocalcin levels; **b** Nonfasting blood glucose; **c** Fasting blood glucose; **d** Blood glucose levels after the glucose loading; **e** Area under the curve in OGTT; **f** Fasting plasma insulin levels; **g** HOMA-IR. Data are expressed as mean ± SEM ($n = 10$). $^{###}P < 0.001$ vs. C57; $^{*}P < 0.05$, $^{**}P < 0.01$, $^{***}P < 0.001$ vs. KKAy

enhanced both hepatic insulin signaling and glycometabolic pathways involved in gluconeogenesis and glycogen synthesis.

Both glycogenolysis and gluconeogenesis lead to hepatic glucose production (HGP), contributing to blood glucose homeostasis, especially in the starving state (FBG). Gluconeogenesis is mainly regulated by insulin, while glycogenolysis is stimulated by glucagon. The data in primary cultured hepatocytes (Fig. 5e, f) showed that GluOC treatment triggered a concentration-dependent inhibition of HGP under both insulin-free and insulin-stimulated conditions. This finding was in accordance with the suppressed hepatic Foxo1 expression without insulin stimulation and the enhanced Foxo1 phosphorylation with insulin stimulation by GluOC treatment in KKAy mice.

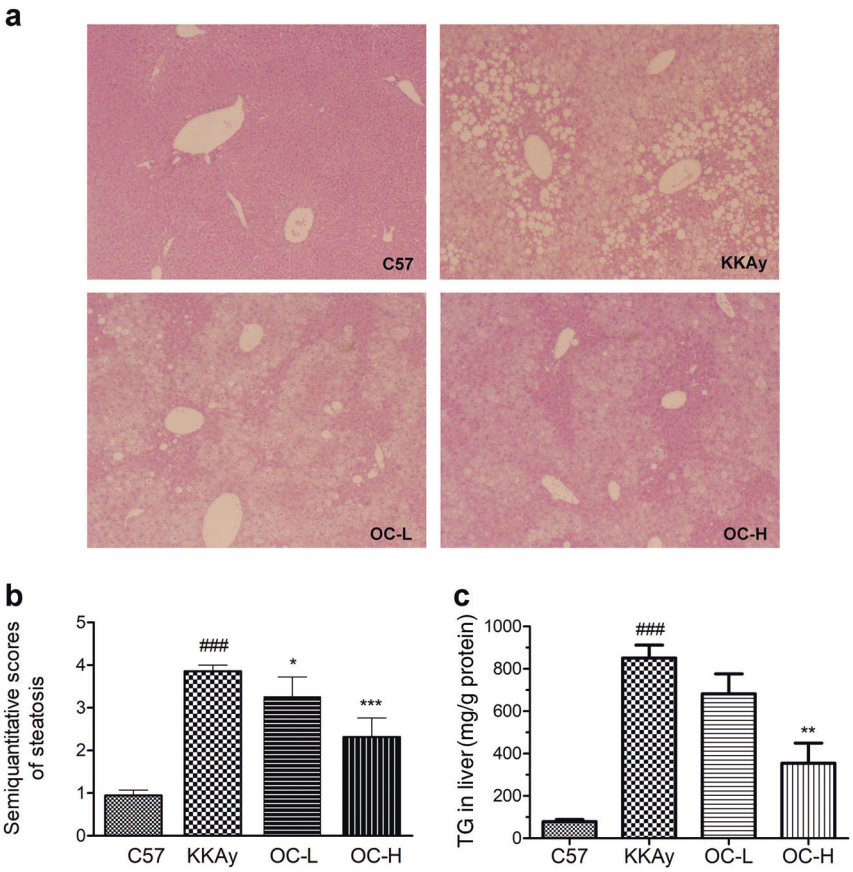

Fig. 2 GluOC treatment prevents hepatic steatosis in KKAy mice. KKAy mice were orally treated with GluOC (3 or 30 ng/g BW) for 4 weeks. At the end of the experiment, liver tissues were collected from the fasted mice for histological and TG content determination. **a** Liver histopathological analysis (H&E stained, 40 ×); **b** Semi-quantitative scoring of steatosis; **c** TG content determination. Data are expressed as mean ± SEM ($n = 5$). $^{###}P < 0.001$ vs. C57; $^{*}P < 0.05$, $^{**}P < 0.01$, $^{***}P < 0.001$ vs. KKAy

The effect of GluOC on glycogen synthesis was also evaluated in primary cultured hepatocytes. As shown in Fig. 5g, h, GluOC promoted insulin-stimulated GSK3β phosphorylation, suggesting that OC could enhance glycogen synthesis in vitro. This result was consistent with the improved nonfasting blood glucose after OC administration in KKAy mice.

GluOC treatment ameliorates hepatic steatosis by inhibiting de novo lipogenesis and enhancing fatty-acid β-oxidation in KKAy mice

Hepatic lipid metabolism pathways, including fatty acid uptake (CD36), fatty-acid β-oxidation (CPT1, MCAD), and de novo lipogenesis (SREBP1c, ACC, FAS), were evaluated by western blot. As shown in Fig. 6a, b, the hepatic expression of SREBP1c and FAS was upregulated in KKAy mice, indicating increased hepatic lipogenesis. Remarkably, hepatic lipogenesis was inhibited by OC treatment, which downregulated the expression of SREBP1c, ACC and FAS, especially in the OC-H group. The fatty-acid β-oxidation in KKAy mice was significantly lower, but it was significantly higher following GluOC treatment (Fig. 6c, d). Interestingly, CD36 expression was upregulated in the GluOC-treated group, which might be compensatory to the decreased de novo lipogenesis.

GluOC treatment changes hepatic fatty-acid metabolic processes in KKAy mice

GO enrichment analysis of the expressed hepatic proteins suggested that the hepatic proteins that were differentially expressed were mainly correlated with biological processes and functions and cellular components (Fig. 7a). Fatty-acid metabolic processes and responses to endoplasmic reticulum stress were strongly affected by GluOC treatment. The representatives of differentially expressed proteins in the fatty-acid metabolic process are shown in Fig. 7b. Interestingly, the hepatic expression of malonyl-CoA-acyl carrier protein transacylase (MCAT) was significantly downregulated by GluOC treatment. Indeed, immunoblot analysis revealed the suppressed hepatic expression of MCAT (Fig. 7c).

DISCUSSION

The liver is the most important organ for glucose and lipid metabolism. Under physiological conditions, the hepatic response to insulin includes inhibition of gluconeogenesis and facilitation of lipogenesis. However, hepatic lipogenesis remains functional while gluconeogenesis is no longer inhibited in the insulin-resistant state. An increased blood insulin level, as a result of failing to bring down blood glucose, continuously favors hepatic lipogenesis, resulting in fat accumulation or steatosis. Thus, insulin resistance is a culprit in the pathogenesis of fatty liver. Previous studies suggested that insulin sensitivity can be improved in adipose tissue and muscle by GluOC administration [15–17]. This study investigated the insulin-sensitizing effect in the liver of KKAy mice. We found that osteocalcin treatment improved hepatic glucose and lipid metabolism, which was likely mediated through activating the insulin signaling pathway.

GluOC enhances hepatic insulin sensitivity in KKAy mice

Insulin functions by activating the insulin receptor and the downstream signaling molecules of the insulin signaling pathway.

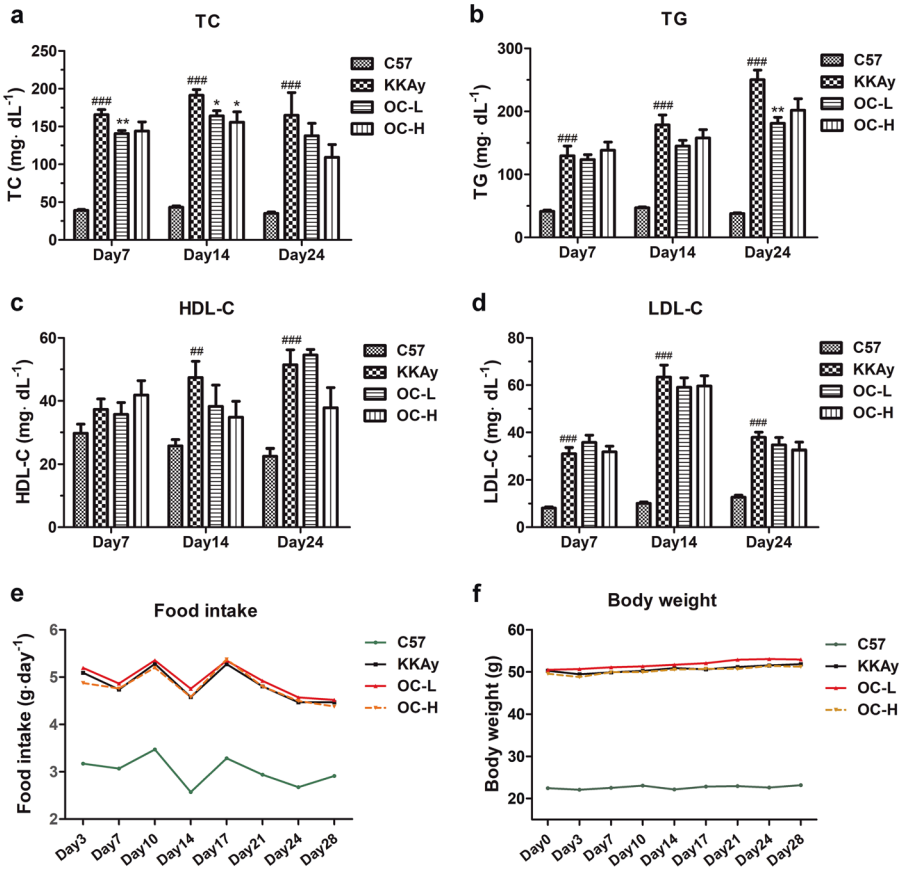

Fig. 3 GluOC teatment ameliorates dyslipidemia in KKAy mice. Animals were treated with GluOC (3 or 30 ng/g BW) for 28 days. **a** Serum TC; **b** Serum TG; **c** Serum HDL-C; **d** Serum LDL-C; **e** Food intake; **f** Body weight. Data are expressed as mean ± SEM ($n = 10$). $^{\#\#}P < 0.01$, $^{\#\#\#}P < 0.001$ vs. C57; $^{*}P < 0.05$, $^{**}P < 0.01$ vs. KKAy

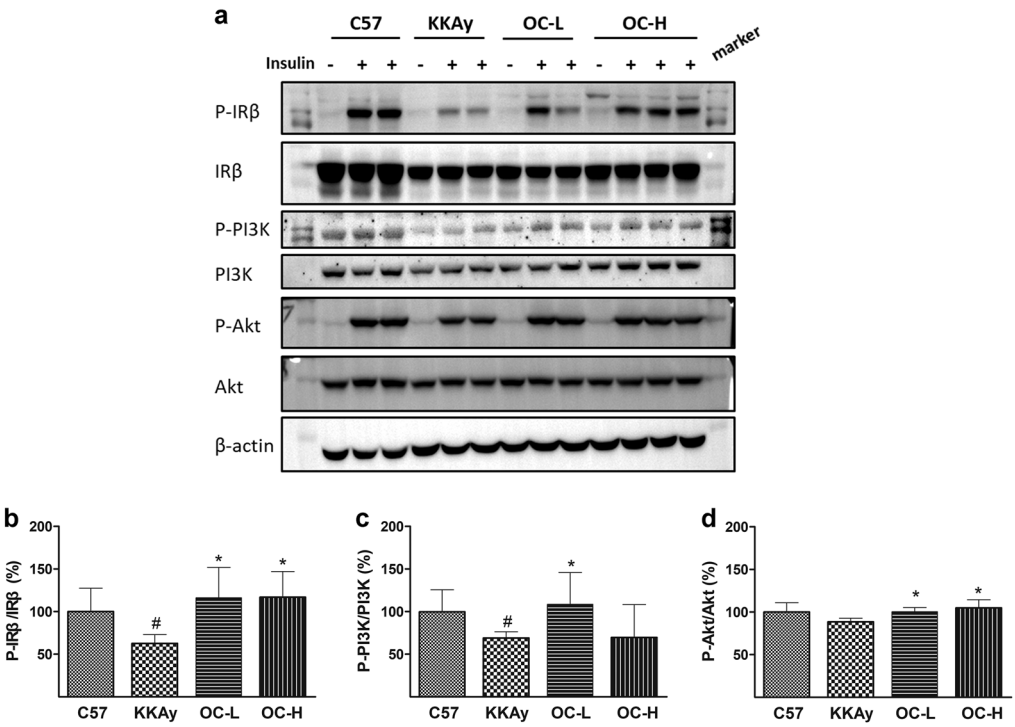

Fig. 4 GluOC treatment increases hepatic insulin sensitivity in KKAy mice. At the end of 4-week GluOC administration (3 or 30 ng/g), animals were fasted overnight, anesthetized, and injected with a bolus of 1 unit/kg of quick-acting insulin or saline via inferior vena cava. Three minutes later, liver tissues were sequentially collected for WB analysis. **a** Phosphorylation of insulin receptor (IRβ), PI3K, and Akt kinases; **b**–**d** Quantification of IRβ, PI3K, and Akt phosphorylation. The targeted protein intensity was quantified by normalizing intensities of phosphorylated proteins to total proteins. Data are expressed as mean ± SD ($n = 4$–5). $^{\#}P < 0.05$ vs. C57; $^{*}P < 0.05$ vs. KKAy

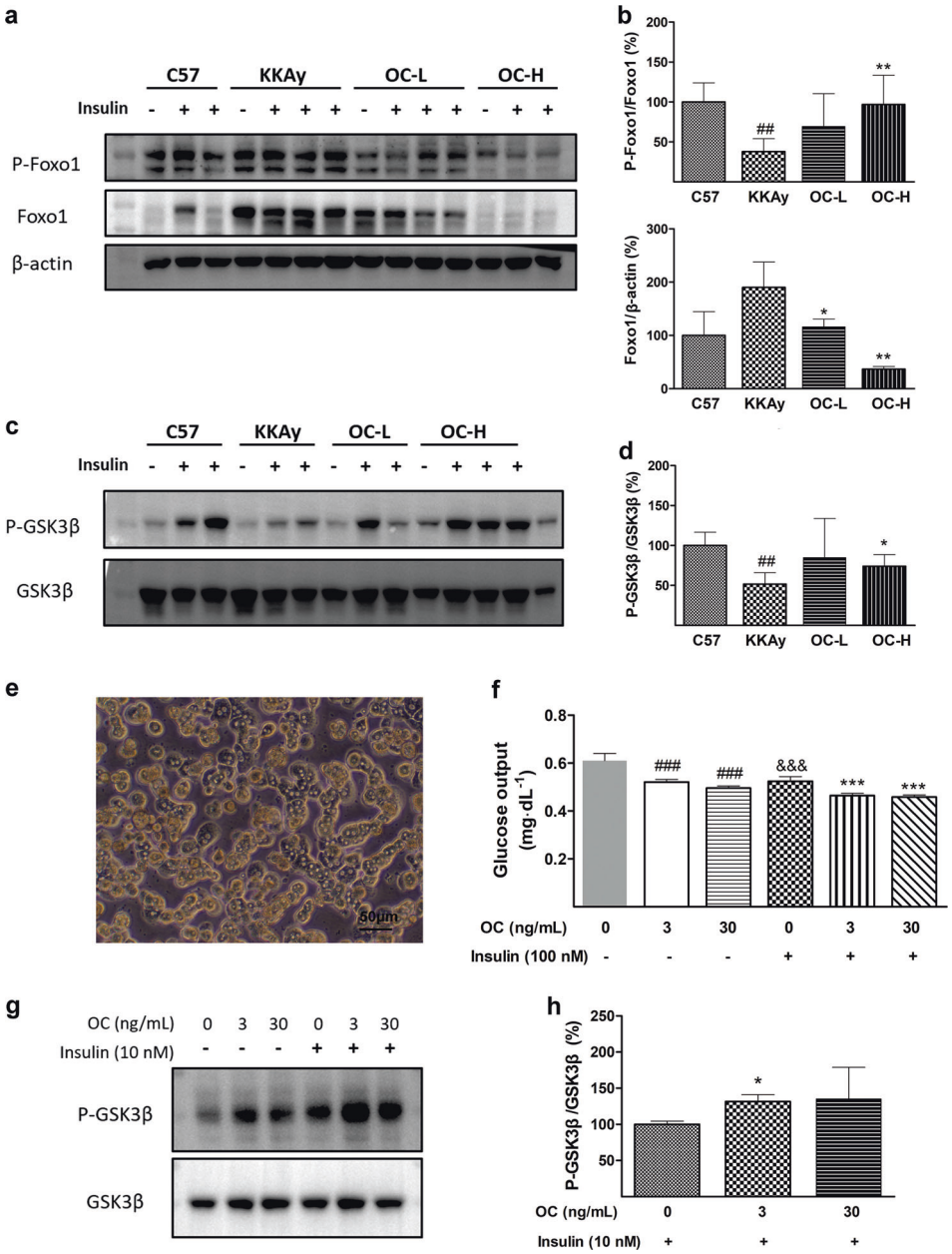

Fig. 5 GluOC treatment regulates hepatic glucose metabolism via suppressing gluconeogenesis and promoting glycogen synthesis. **a**–**d** GluOC regulates hepatic glycometabolic pathways in KKAy mice. At the end of 4-week GluOC administration (3 or 30 ng/g), animals were fasted overnight, anesthetized, and injected with a bolus of 1 unit/kg of quick-acting insulin or saline via inferior vena cava. Three minutes later, liver tissues were sequentially collected for WB analysis. **a** Phosphorylation of Foxo1; **b** Quantification of total Foxo1 and phosphorylation; **c** Phosphorylation of GSK3β; **d** Quantification of GKS3β phosphorylation. The immunoblot data were quantified by normalizing intensities of phosphorylated proteins to total proteins. Data are expressed as mean ± SD ($n = 4$–5). $^{\#\#}P < 0.01$ vs. C57; $^{*}P < 0.05$, $^{**}P < 0.01$ vs. KKAy. **e** and **f** GluOC inhibits glucose output in primary cultured hepatocytes. Primary hepatocytes were isolated from male C57BL/6 mice, seeded in six-well plate in William's E medium for 24 h, and starved for 4 h; then cells were treated with GluOC for 24 h, washed with PBS, and incubated in glucose- and phenol red-free medium containing 2 mM sodium pyruvate, 20 mM sodium lactate for 4 h. The medium was withdrawn for measure of glucose concentration. **e** Images of primary cultured hepatocytes 24 h after seeding; **f** Glucose output was suppressed by GluOC. Data are expressed as mean ± SD ($n = 6$). $^{\#\#\#}P < 0.001$ vs. 0 ng/mL in insulin-free group; $^{\&\&\&}P < 0.001$ vs. 0 ng/mL in insulin-free group; $^{***}P < 0.001$ vs. 0 ng/mL in insulin-stimulated group. **g**, **h** GluOC promotes GSK3β phosphorylation in primary cultured hepatocytes. Cells were serum-starved for 6 h, and then treated with GluOC (0, 3, 30 ng/mL) for 24 h followed by 10 nM insulin treatment for 5 min. The phosphorylation of GSK3β was determined by immunoblotting. **g** Phosphorylation of GSK3β; **h** Quantification of GSK3β phosphorylation. Data are expressed as mean ± SD ($n = 3$). $^{*}P < 0.05$ vs. 0 ng/mL in insulin-stimulated group

The binding of insulin to insulin receptor (IR) triggers phosphorylation of insulin receptor β (IRβ) and its substrate (IRS), which activates the phosphatidylinositol 3-kinase (PI3K)–Akt/protein kinase B (PKB) pathway, contributing to glucose uptake, glycogen synthesis, and inhibition of gluconeogenesis [29, 30]. In this study, both hyperinsulinemia and the elevated HOMA-IR index in KKAy mice were reduced by GluOC treatment (Fig. 1f, g). In OGTT, the IGT was also improved (Fig. 1d, e). Thus, GluOC treatment mitigated hepatic insulin resistance, as evidenced by the increased hepatic insulin-stimulated phosphorylation of IRβ, PI3K, and Akt (Fig. 4).

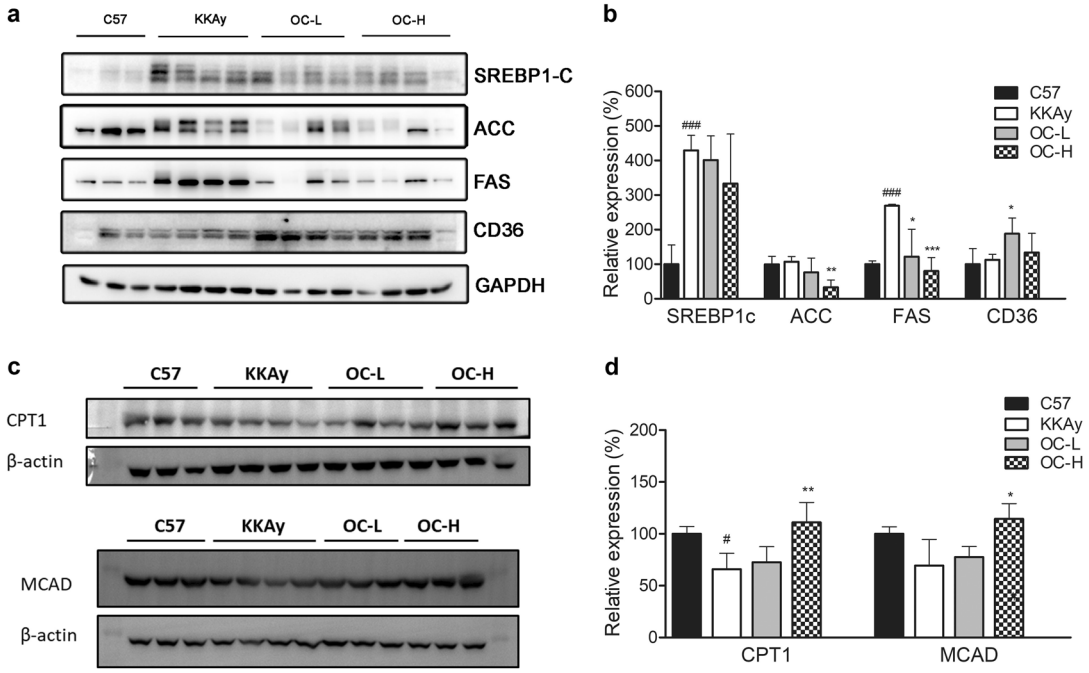

Fig. 6 GluOC treatment ameliorates hepatic steatosis via inhibiting de novo lipogenesis and enhancing fatty-acid β-oxidation in KKAy mice. KKAy mice were orally treated with GluOC (3 or 30 ng/g) for 4 weeks. At the end of experiment, mice were fasted overnight and anesthetized, and liver tissues were collected for protein analysis. **a** and **b** Expression levels of SREBP1c, ACC, FAS, CD36, and GAPDH by immunoblot; **c** and **d** Expression levels of CPT1, MCAD, and β-actin. The immunoblot data were quantified by normalizing intensity of each protein to GAPDH or β-actin. Data are expressed as mean ± SD ($n = 3$–4). $^{\#}P < 0.05$, $^{\#\#\#}P < 0.001$ vs. C57; $^{*}P < 0.05$, $^{**}P < 0.01$, $^{***}P < 0.001$ vs. KKAy

GluOC ameliorates hyperglycemia through the glycometabolic pathway in KKAy mice

Fasting blood glucose (FBG) was significantly improved in the GluOC-treated group. However, the decrease in nonfasting blood glucose was not as efficient as FBG (Fig. 1b, c). FBG is mainly maintained by hepatic glycogenolysis and gluconeogenesis, while nonfasting blood glucose is mainly regulated by the utilization of glucose by muscle/adipose tissues and glycogen synthesis in liver. In type 2 diabetes mellitus, augmented gluconeogenesis leads to higher blood glucose (especially FBG) and is also a therapeutic target for type 2 diabetes. It is assumed that the liver is the main target organ of GluOC, resulting in increasing hepatic insulin sensitivity, inhibiting HGP and lowering FBG level. Hepatic gluconeogenesis is regulated by Foxo1, and glycogen synthesis is regulated by GSK3β. Insulin normally suppresses hepatic Foxo1 function by activating the protein kinase Akt, which phosphorylates Foxo1, which remains inactive in the cytoplasm [31]. In this study, GluOC treatment increased the insulin-induced phosphorylation of Foxo1 (Fig. 5a, b), which suppressed gluconeogenesis, as demonstrated by the hepatic glucose output assays of the primary cultured hepatocytes (Fig. 5e, f). This explains the significantly decreased FBG in GluOC-treated KKAy mice (Fig. 1c). As expected, the hepatic Foxo1 expression in KKAy mice was significantly higher before GluOC treatment and lower after it treatment compared with C57 mice (Fig. 5b). As reported, a higher hepatic Foxo1 level was an indication of insulin resistance in obese mice, leading to augmented hepatic gluconeogenesis [32, 33]. The suppressed Foxo1 expression could be a mechanism for the observed hypoglycemic effect of GluOC treatment. Insulin also induces GSK3β phosphorylation and inactivation, consequently leading to decreased phosphorylation and increased activation of glycogen synthase (GS). This step is rate-limiting for glycogen synthesis [34]. In this study, the insulin-induced phosphorylation of GSK3β was significantly higher both in GluOC-treated mice liver (Fig. 5c, d) and in primary cultured hepatocytes (Fig. 5g, h), suggesting the promotion of glycogen synthesis and the reduction of nonfasting blood glucose by GluOC administration.

GluOC ameliorates hepatic steatosis by regulating hepatic de novo lipogenesis (DNL) and enhancing fatty-acid β-oxidation in KKAy mice

Insulin resistance is implicated in the pathogenesis of fatty liver [4, 35, 36]. Hepatic steatosis, an early stage of NAFLD, reflects imbalanced lipid storage and lipid secretion, leading to increased lipid accumulation in the liver. Lipid storage includes both the uptake of free fatty acids and DNL in the liver. The pancreas senses insulin resistance by increasing insulin production, which results in hyperinsulinemia. The increased insulin level increases DNL, resulting in steatosis if the lipids cannot be efficiently secreted [37]. DNL can be regulated at the transcriptional level by sterol regulatory element binding protein-1c (SREBP1c) [37–40]. Both insulin and hyperinsulinemia upregulate SEREBP1c expression via multiple insulin signaling pathways, such as mTORC1, PI3K-Akt, and others [4, 41, 42].

In this study, we revealed that GluOC ameliorated steatosis by regulating hepatic de novo lipogenesis (DNL) in KKAy mice

Consistent with the elevated FPI, hepatic SREBP1c expression was increased by 4–5-fold and was accompanied by elevated DNL in KKAy mice compared with C57 mice (Fig. 6a, b). GluOC treatment led to the reduction of both FPI and hepatic SREBP1c expression, suggesting that GluOC ameliorated hyperinsulinemia (Fig. 1f) and then suppressed SREBP1c expression. We further determined the expression levels of acetyl-CoA carboxylase (ACC) and fatty-acid synthase (FAS), two main enzymes involved in DNL. SREBP1c has been reported to activate ACC and FAS [43–45]. In this study, ACC and FAS expression was reduced in the GluOC treatment group, which was consistent with the decreased SREBP1c expression, indicating that GluOC improved hepatic steatosis by suppressing hepatic DNL in KKAy mice. Additionally, hepatic CPT1 and MCAD expression were both initially lower and then became significantly

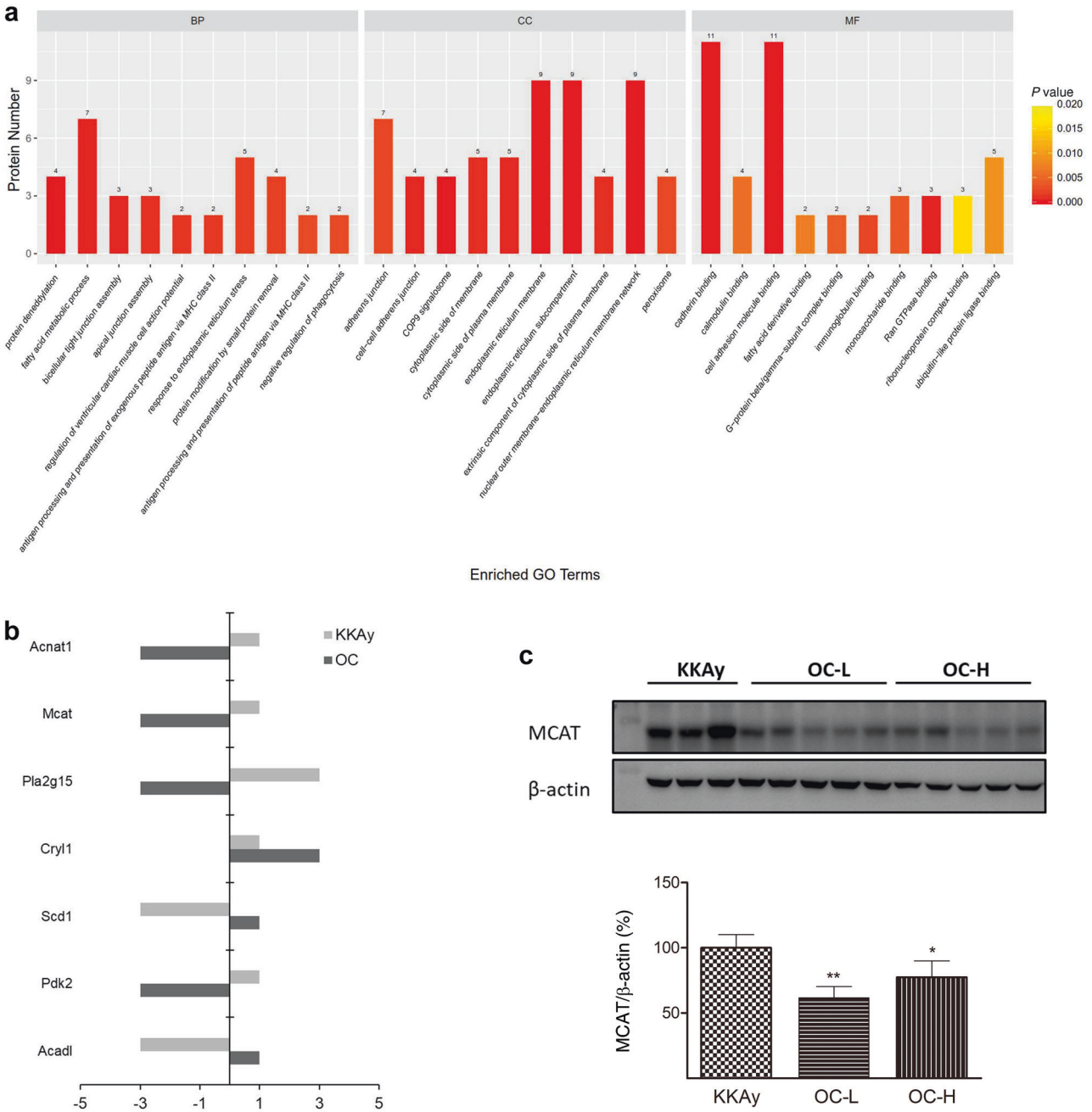

Fig. 7 GluOC treatment changes hepatic fatty-acid metabolic process in KKAy mice. **a** Comparison of the GO analysis of the proteins between the OC-treated mice and non-OC-treated KKAy mice. Comparison is summarized as the following three GO terms: Biological processes (BP), cellular compartments (CC), and molecular functions (MF); **b** Changes in the representative fatty-acid metabolic process-associated proteins (OC-L vs. KKAy); **c** Hepatic expression of MCAT by immunoblot. Data are expressed as mean ± SD ($n = 3–5$). *$P < 0.05$, **$P < 0.01$ vs. KKAy

higher after GluOC treatment in KKAy mice compared to C57 mice (Fig. 6c, d). CPT1 is a regulatory enzyme in the mitochondria that transfers FAs from the cytosol to the mitochondria prior to β-oxidation [46]. Medium-chain acyl-CoA dehydrogenase (MCAD) participates in the first reaction of mitochondrial fatty-acid β-oxidation, catalyzing C4 to C12 straight-chain acyl-CoAs [47]. These results imply that GluOC treatment could augment fatty-acid β-oxidation to mitigate steatosis.

GluOC ameliorates dyslipidemia partly by suppressing hepatic DNL in KKAy mice

Blood TG level is mainly affected by exogenous food intake and endogenous liver synthesis. As shown in Fig. 3, the food intake remained unchanged during GluOC administration. The improved hypertriglyceridemia might be attributed to the suppressed DNL and the reduced hepatic TG synthesis and steatosis. Hypercholesterolemia in KKAy mice was also improved, though the mechanisms are unknown at this time.

Interestingly, proteomic analysis indicated that GluOC downregulated MCAT expression

MCAT is required for mitochondrial fatty-acid synthesis (FASII) and is implicated in insulin resistance and gestational diabetes mellitus [48]. This protein is exclusively expressed in the mitochondrion, where the enzymatic function transfers a malonyl group from malonyl-CoA to mitochondrial acyl carrier protein [49]. The LC-MS/

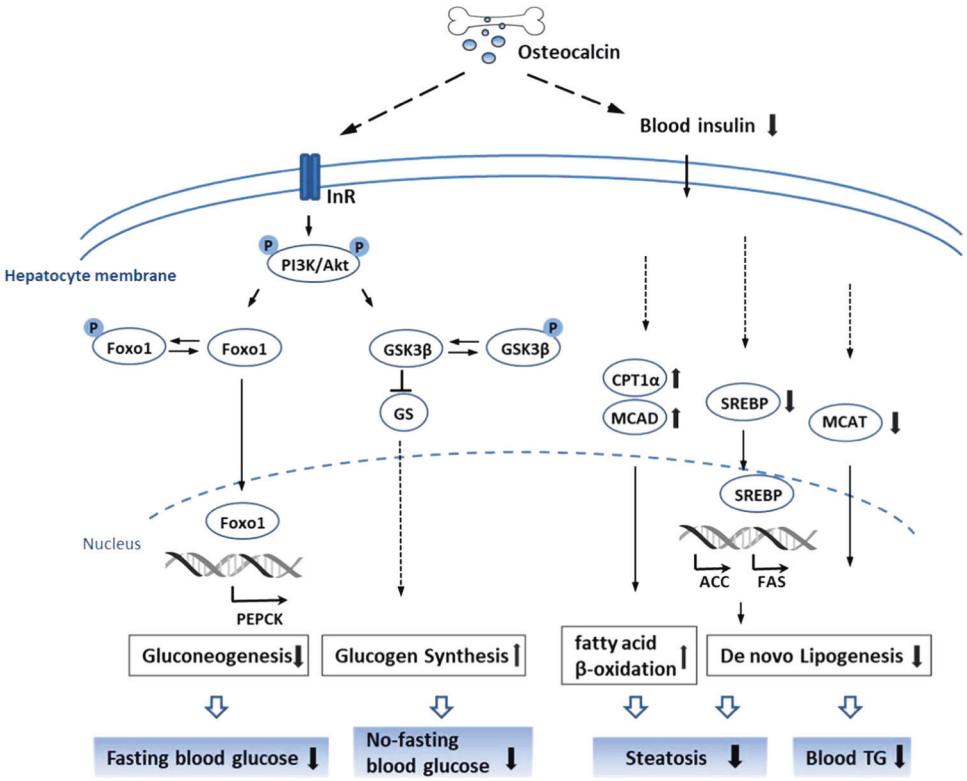

Fig. 8 Proposed mechanisms for the GluOC therapeutic effects on hyperglycemia and hepatic steatosis in KKAy mice

MS analysis of mouse liver samples suggested that GluOC treatment significantly reduced MCAT expression, affecting the fatty-acid metabolic process (Fig. 7) and contributing to the decreased DNL and the ameliorated steatosis.

According to the literature and our experimental results, oral administration is safe, effective, and convenient. Previous studies reported that oral osteocalcin could enter the circulation. Mizokami et al. [50] showed that oral administration of osteocalcin was as effective as the intraperitoneal route in increasing the serum concentration of insulin in mice. Another study [17] showed that 4 weeks of daily oral administration of osteocalcin (10 ng/g) significantly increased the serum OC. In our study, the blood uncarboxylated OC levels were elevated after a 14-day OC administration (Fig. 1a). Some studies also suggested that oral administration of OC might exert metabolic regulation by stimulating the release of GLP-1 from the intestine. However, no side effects of GLP-1 analogs were observed in this study, such as appetite suppression or body weight decrease (as shown in Fig. 3). Therefore, we speculate that GluOC may play a direct role in hepatic glucose and lipid metabolism by being absorbed into the blood circulation. The in-depth mechanism needs to be further studied.

In conclusion, this study provides preliminary but encouraging evidence that GluOC treatment improved hyperglycemia, hepatic steatosis, and dyslipidemia in KKAy mice and suggests that GluOC is a promising drug candidate for metabolic syndrome treatment. The uncovered GluOC hypoglycemic mechanisms included enhancing the insulin signaling pathway, increasing hepatic Foxo1/GSK3β phosphorylation and regulating hepatic glucose metabolism. The reduced blood insulin level and hepatic SREBP1c/ACC/FAS and MCAT expression likely contributed to hepatic lipid reduction by inhibiting de novo lipogenesis, together with the elevated fatty-acid β-oxidation, as evidenced by the ameliorated hyperlipidemia in KKAy mice (Fig. 8).

ACKNOWLEDGEMENTS

This work was supported by the grant for a combined research and teaching program from the College of Life Sciences, University of Chinese Academy of Sciences (KJRH2015-006). We also thank the support of the CAMS Innovation Fund for Medical Sciences (CIFMS-2016-I2M-3-012) and the Drug Innovation Major Project (2018ZX09711001-003-005).

AUTHOR CONTRIBUTIONS

XLZ and YNW conducted the pharmacological experiments; LYM and ZSL prepared uncarboxylated osteocalcin; XLZ, FY, and JHY designed the study, integrated the data, and wrote the manuscript.

ADDITIONAL INFORMATION

Competing interests: The authors declare no competing interests.

REFERENCES

1. Crespo M, Lappe S, Feldstein AE, Alkhouri N. Similarities and differences between pediatric and adult nonalcoholic fatty liver disease. Metabolism. 2016;65:1161–71.
2. Machado M, Cortez-Pinto H. Non-alcoholic steatohepatitis and metabolic syndrome. Curr Opin Clin Nutr Metab Care. 2006;9:637–42.
3. Asrih M, Jornayvaz FR. Metabolic syndrome and nonalcoholic fatty liver disease: Is insulin resistance the link? Mol Cell Endocrinol. 2015;418(Pt 1):55–65.
4. Alam S, Mustafa G, Alam M, Ahmad N. Insulin resistance in development and progression of nonalcoholic fatty liver disease. World J Gastrointest Pathophysiol. 2016;7:211–7.
5. Tanaka N, Kimura T, Fujimori N, Nagaya T, Komatsu M, Tanaka E. Current status, problems, and perspectives of non-alcoholic fatty liver disease research. World J Gastroenterol. 2019;25:163–77.
6. Yki-Jarvinen H. Non-alcoholic fatty liver disease as a cause and a consequence of metabolic syndrome. Lancet Diabetes Endocrinol. 2014;2:901–10.
7. Basaranoglu M. Understanding mechanisms of the pathogenesis of nonalcoholic fatty liver disease. World J Gastroenterol. 2010;16:2223.

8. Takamura T, Misu H, Ota T, Kaneko S. Fatty liver as a consequence and cause of insulin resistance: lessons from type 2 diabetic liver. Endocr J. 2012;59:745–63.
9. Hong F, Xu P, Zhai Y. The opportunities and challenges of peroxisome proliferator-activated receptors ligands in clinical drug discovery and development. Int J Mol Sci. 2018;19:2189.
10. Tang Y, Zhang X, Chen Z, Yin W, Nan G, Tian J, et al. Novel benzamido derivatives as PTP1B inhibitors with anti-hyperglycemic and lipid-lowering efficacy. Acta Pharm Sin B. 2018;8:919–32.
11. Zoch ML, Clemens TL, Riddle RC. New insights into the biology of osteocalcin. Bone. 2016;82:42–9.
12. Lee NK, Sowa H, Hinoi E, Ferron M, Ahn JD, Confavreux C, et al. Endocrine regulation of energy metabolism by the skeleton. Cell. 2007;130:456–69.
13. Patti A, Gennari L, Merlotti D, Dotta F, Nuti R. Endocrine actions of osteocalcin. Int J Endocrinol. 2013;2013:846480.
14. Pi M, Chen L, Huang MZ, Zhu W, Ringhofer B, Luo J, et al. GPRC6A null mice exhibit osteopenia, feminization and metabolic syndrome. PLoS One. 2008;3:e3858.
15. Ferron M, Hinoi E, Karsenty G, Ducy P. Osteocalcin differentially regulates beta cell and adipocyte gene expression and affects the development of metabolic diseases in wild-type mice. Proc Natl Acad Sci U S A. 2008;105:5266–70.
16. Ferron M, McKee MD, Levine RL, Ducy P, Karsenty G. Intermittent injections of osteocalcin improve glucose metabolism and prevent type 2 diabetes in mice. Bone. 2012;50:568–75.
17. Mizokami A, Yasutake Y, Higashi S, Kawakubo-Yasukochi T, Chishaki S, Takahashi I, et al. Oral administration of osteocalcin improves glucose utilization by stimulating glucagon-like peptide-1 secretion. Bone. 2014;69:68–79.
18. Guedes JAC, Esteves JV, Morais MR, Zorn TM, Furuya DT. Osteocalcin improves insulin resistance and inflammation in obese mice: Participation of white adipose tissue and bone. Bone. 2018;115:68–82.
19. Gupte AA, Sabek OM, Fraga D, Minze LJ, Nishimoto SK, Liu JZ, et al. Osteocalcin protects against nonalcoholic steatohepatitis in a mouse model of metabolic syndrome. Endocrinology. 2014;155:4697–705.
20. Yamamoto T, Yamaguchi H, Miki H, Shimada M, Nakada Y, Ogino M, et al. Coenzyme a: diacylglycerol acyltransferase 1 inhibitor ameliorates obesity, liver steatosis, and lipid metabolism abnormality in KKAy mice fed high-fat or high-carbohydrate diets. Eur J Pharmacol. 2010;640:243–9.
21. Fu C, Zhang X, Ye F, Yang J. High insulin levels in KK-Ay diabetic mice cause increased cortical bone mass and impaired trabecular micro-structure. Int J Mol Sci. 2015;16:8213–26.
22. Han TS, Sattar N, Williams K, Gonzalez-Villalpando C, Lean ME, Haffner SM. Prospective study of C-reactive protein in relation to the development of diabetes and metabolic syndrome in the Mexico City Diabetes Study. Diabetes Care. 2002;25:2016–21.
23. Shi QZ, Wang LW, Zhang W, Gong ZJ. Betaine inhibits toll-like receptor 4 expression in rats with ethanol-induced liver injury. World J Gastroenterol. 2010;16:897–903.
24. Bligh EG, Dyer WJ. A rapid method of total lipid extraction and purification. Can J Biochem Physiol. 1959;37:911–7.
25. Ma YM, Tao RY, Liu Q, Li J, Tian JY, Zhang XL, et al. PTP1B inhibitor improves both insulin resistance and lipid abnormalities in vivo and in vitro. Mol Cell Biochem. 2011;357:65–72.
26. Liu HY, Collins QF, Xiong Y, Moukdar F, Lupo EG Jr., Liu Z, et al. Prolonged treatment of primary hepatocytes with oleate induces insulin resistance through p38 mitogen-activated protein kinase. J Biol Chem. 2007;282:14205–12.
27. Wisniewski JR, Zougman A, Nagaraj N, Mann M. Universal sample preparation method for proteome analysis. Nat Methods. 2009;6:359–62.
28. Tyanova S, Temu T, Carlson A, Sinitcyn P, Mann M, Cox J. Visualization of LC-MS/MS proteomics data in MaxQuant. Proteomics. 2015;15:1453–6.
29. Biddinger SB, Kahn CR. From mice to men: insights into the insulin resistance syndromes. Annu Rev Physiol. 2006;68:123–58.
30. White MF. Insulin signaling in health and disease. Science. 2003;302:1710–1.
31. Gross DN, van den Heuvel AP, Birnbaum MJ. The role of FoxO in the regulation of metabolism. Oncogene. 2008;27:2320–36.
32. Titchenell PM, Quinn WJ, Lu M, Chu Q, Lu W, Li C, et al. Direct hepatocyte insulin signaling is required for lipogenesis but is dispensable for the suppression of glucose production. Cell Metab. 2016;23:1154–66.
33. Qu S, Altomonte J, Perdomo G, He J, Fan Y, Kamagate A, et al. Aberrant forkhead box O1 function is associated with impaired hepatic metabolism. Endocrinology. 2006;147:5641–52.
34. Shepherd PR, Withers DJ, Siddle K. Phosphoinositide 3-kinase: the key switch mechanism in insulin signalling. Biochem J. 1998;333(Pt 3):471–90.
35. Gruben N, Shiri-Sverdlov R, Koonen DP, Hofker MH. Nonalcoholic fatty liver disease: a main driver of insulin resistance or a dangerous liaison? Biochim Biophys Acta. 2014;1842:2329–43.
36. Bugianesi E, Moscatiello S, Ciaravella MF, Marchesini G. Insulin resistance in nonalcoholic fatty liver disease. Curr Pharm Des. 2010;16:1941–51.
37. Konner AC, Bruning JC. Selective insulin and leptin resistance in metabolic disorders. Cell Metab. 2012;16:144–52.
38. Paschos P, Paletas K. Non alcoholic fatty liver disease and metabolic syndrome. Hippokratia. 2009;13:9–19.
39. Sanyal AJ. Mechanisms of disease: pathogenesis of nonalcoholic fatty liver disease. Nat Clin Pr Gastroenterol Hepatol. 2005;2:46–53.
40. Wang Y, Viscarra J, Kim SJ, Sul HS. Transcriptional regulation of hepatic lipogenesis. Nat Rev Mol Cell Biol. 2015;16:678–89.
41. Shao W, Espenshade PJ. Expanding roles for SREBP in metabolism. Cell Metab. 2012;16:414–9.
42. Wong RH, Sul HS. Insulin signaling in fatty acid and fat synthesis: a transcriptional perspective. Curr Opin Pharmacol. 2010;10:684–91.
43. Horton JD, Goldstein JL, Brown MS. SREBPs: activators of the complete program of cholesterol and fatty acid synthesis in the liver. J Clin Investig. 2002;109:1125–31.
44. Magana MM, Koo SH, Towle HC, Osborne TF. Different sterol regulatory element-binding protein-1 isoforms utilize distinct co-regulatory factors to activate the promoter for fatty acid synthase. J Biol Chem. 2000;275:4726–33.
45. Lopez JM, Bennett MK, Sanchez HB, Rosenfeld JM, Osborne TF. Sterol regulation of acetyl coenzyme A carboxylase: a mechanism for coordinate control of cellular lipid. Proc Natl Acad Sci U S A. 1996;93:1049–53.
46. Huang YY, Gusdon AM, Qu S. Nonalcoholic fatty liver disease: molecular pathways and therapeutic strategies. Lipids Health Dis. 2013;12:171.
47. Matsubara Y, Kraus JP, Yang-Feng TL, Francke U, Rosenberg LE, Tanaka K. Molecular cloning of cDNAs encoding rat and human medium-chain acyl-CoA dehydrogenase and assignment of the gene to human chromosome 1. Proc Natl Acad Sci U S A. 1986;83:6543–7.
48. Zhang Y, Ye J, Fan J. Regulation of malonyl-CoA-acyl carrier protein transacylase network in umbilical cord blood affected by intrauterine hyperglycemia. Oncotarget. 2017;8:75254–63.
49. Zhang L, Joshi AK, Smith S. Cloning, expression, characterization, and interaction of two components of a human mitochondrial fatty acid synthase. Malonyltransferase and acyl carrier protein. J Biol Chem. 2003;278:40067–74.
50. Mizokami A, Yasutake Y, Gao J, Matsuda M, Takahashi I, Takeuchi H, et al. Osteocalcin induces release of glucagon-like peptide-1 and thereby stimulates insulin secretion in mice. PLoS One. 2013;8:e57375.